Load rejection transient with joint closing law of ball-valve and guide vane for two units in pumped storage power station

Xiaoqin Li, Xuelin Tang, Xiaoyan Shi, Honghao Chen and Changsheng Li

ABSTRACT

It is more dangerous for the units sharing the same division pipeline system than those sharing individual system during the load rejection transient for a high water head pumped storage station. A new mathematical model for the load rejection transient in these two units sharing the same division pipeline was proposed using method of internal characteristic (MIC). The transient relationship between the geometric parameters and working parameters was established based on the dynamic equations of the hydraulic machinery. Meanwhile, the calculation of the load rejection transient was accomplished and compared with field experimental data from a pumped storage power station. The relative errors of the maximum rotational speed of the two units between the predicted results and the experimental data were −5.9% and −4.44%, respectively, and the relative errors of the maximum rising of hydraulic pressure were −6.7% and −6.98%, respectively. The results met with the design specification requirements, which indicated that the proposed new MIC could completely predict the load rejection transient in these two units with joint closing law of ball-valve and guide vane, and the corresponding calculated results were acceptable and reliable. The MIC is also applicable to the transient investigation of hydraulic systems with hydraulic machinery.

Key words | ball-valve, joint closing law, load rejection transient, method of internal characteristic, pumped storage power station

Xiaoqin Li (corresponding author)
Xuelin Tang
Xiaoyan Shi
Beijing Engineering Research Center of Safety and
    Energy Saving Technology for Water Supply
    Network System,
Beijing 100083,
China
and
College of Water Resources and Civil Engineering,
China Agricultural University,
Beijing 100083,
China
E-mail: mlp84238@163.com

Honghao Chen
Shenzhen Pumped Storage Co., Ltd, Power
    Generation Company, CSG,
Shenzhen 518000,
China

Changsheng Li
Henan Tianchi Pumped Storage Co., Ltd,
Nanyang 473000,
China

NOMENCLATURE

M	Moment, N·m	v_{u2}	Circumference component of absolute velocity at outlet, m
ρ	Fluid mass density, kg/m^3	r_1	Inlet radius of pump-turbine, m
W	Volume, m^3	r_2	Outlet radius of pump-turbine, m
b	Infinitesimal thickness, m	M_H	Transient moment acting on runner, N·m
θ	Infinitesimal angle, °	Q_H	Transient flow discharge, m^3/s
m	Infinitesimal axial meridian, m	H_H	Turbine transient water head, m
r	Radius of micro fluid to center of shaft, m	g	Gravitational acceleration, m/s^2
v_u	Circumference component of absolute velocity, m/s	η	Hydraulic efficiency
t	Time, s	ω_H	Transient angular speed, rad/s
v_m	Axial meridian velocity, m/s	H_{eH}	Transient effective water head, m
Q	Flow discharge, m^3/s	u_1	Circumference velocity at inlet, m/s
v_{u1}	Circumference component of absolute velocity at inlet, m/s	u_2	Circumference velocity at outlet, m/s

Γ_1	Velocity circulation at inlet, m²/s
Γ_2	Velocity circulation at outlet, m²/s
α	Angle between outlet of guide vane and circumferential direction, °
b_0	Height of guide vane, m
K_p	Cascade transparent coefficient
l	Length of hydrofoil of cascade, m
t_c	Pitch of hydrofoil of cascade, m
r_a	Effective radius of runner cascade, m
i_0	Coefficient of cascade in zero lift force
β_2	Blade angle at outlet of meridian plane of runner, °
F	Area, m²
q	Flow discharge of layer thickness, m³/s
v_r	Radial component of absolute velocity, m/s
ω	Angular speed of unit, rad/s
M_D	Driving moment, N·m
M_R	Resisting moment, N·m
J	Inertia moment of rotating parts, kg·m²
G	Weight of rotating parts, N
D	Distance from center of mass of rotating parts to axle, m
ω_0	Initial angular speed, rad/s
K	Mockridge shaft moment coefficient
M_M	Mockridge moment, N·m
b_p	Blade width at outlet of pump, m
D_p	Runner diameter at outlet of pump, m
n	Rotational speed of unit, r/min
Y_{ul}	Water level of upstream reservoir, m
a_w	Wave velocity, m/s
A	Cross-sectional area of pipe, m²
H_P	Transient water head in P point, m
Q_p	Transient flow discharge in P point, m
H_{v0}	Initial pressure at inlet of ball-valve at full opening, m
ξ	Pressure rising rate
Q_{cb}	Static flow discharge of ball-valve, m³/s
Δx	Space increment, m
f	Darcy–Weisbach friction factor
Q_c	Static flow discharge, m³/s
y	Relative guide vane opening
Q_0	Static flow discharge at full opening of guide vane, m³/s
a	Guide vane opening, °
a_0	Full opening of guide vane, °
k	Exponent
H_{zp}	Transient water head of device, m

H_{z0}	Static water head of device, m
D_1	Runner diameter of pump-turbine, m
n_H	Transient rotational speed, r/min
n_0	Initial rotational speed, r/min
k_q	Rate of change of unit discharge with respect to unit speed
H_0	Static water head at spiral case inlet, m
σ_T	Characteristic coefficient of draft tube
L_{dr}	Length of draft tube, m
v_{dr}	Initial average velocity in draft tube, m/s
t_s	Closing time of guide vane, s
b_0	Height of guide vane, m
K_1	Iterative coefficient
c_1	Coefficient
c_2	Coefficient
K_2	Coefficient
Q_T	Flow discharge at outlet of downstream surge tank, m³/s
Q_S	Flow discharge of downstream surge tank, m³/s
hs	Depth of downstream surge tank, m
H_{dS}	Water head of downstream surge tank, m
H_{S0}	Water head at bottom of downstream surge tank, m
f_S	Friction factor of downstream surge tank
D_S	Diameter of downstream surge tank, m
A_S	Cross-sectional area of downstream surge tank, m²
Y_{dl}	Water level of downstream reservoir, m

INTRODUCTION

During load rejection transients, the sharp increment and the fluctuation of pipe pressure endanger the safety of the pumped storage power station (Calamak & Bozkus 2013), especially for two units sharing the same diversion pipeline (Yu *et al.* 2014). The 'S' and hump areas in full characteristic curves cause the unsteady dynamic process of pump-turbines with low specific speed under the transient process (Li *et al.* 2016; Zeng *et al.* 2017). Since the negative installation elevation of a draft tube is usually designed to prevent it from cavitation for high water head pumped storage power station, the pressure at the inlet of the draft tube will be much lower when load rejection occurs, which

may cause reverse water hammer in the draft tube and result in huge damage of the device.

Developing a reasonable closing law of guide vanes is an effective method to reduce the pressure pulsation and the rotational speed increment (Fang & Koutnik 2012). Yao *et al.* (2013) investigated the key effect factor for the load rejection in pump-turbines by comparing five different guide closing laws. Vakil & Firoozabadi (2009) analyzed the effect of different multi-line closing laws, and found an optimum closing law for pressure pulsation reduction. The closing law based on ball-valve and guide vane was applied for the load rejection in a pumped storage power station (Zhang & Yang 2011). A numerical simulation of the closing law based on ball-valve and guide vane was adopted by Hou & Cheng (2005), where the results proved that the closing law can ensure the safety of the unit during load rejection. However, more tests were still required to figure out the effects of the closing law on pump-turbine units using joint adjustment of ball-valve and guide vane during load rejection. The one-dimensional method of characteristics (MOC) is widely used in analyzing the transient flow for pipeline systems due to its high efficiency (Freni *et al.* 2013; Acosta *et al.* 2015). Hwang *et al.* (2012) developed a novel particle method of characteristics to simulate unsteady pipe flows and the method was validated by solving some benchmark problems with significant transient effects in single pipe flows. Based on the MOC and the modified Suter transformations, Rezghi & Riasi (2016) simulated the simultaneous operation of two units at runaway.

The transition process of hydraulic machinery should consider unsteady flow characteristics in the hydraulic machinery while the traditional method employs the steady characteristics. The previous investigations on transient are applied with the method of external characteristics, which is based on the full characteristic curves of pump-turbines (Wylie & Streeter 1993; Rezghi & Riasi 2016). However, when the full characteristic curves obtained from a model turbine test in steady state are employed to calculate the transient state, this technique will cause an error. At the same time, the study on the closing law is insufficient, and its influence on dynamic performance in the transition should be further studied.

In this paper, the double units' load rejection transient with the joint closing law of ball-valve and guide vane was calculated for a pumped storage power station. The numerical simulation of double load rejection was carried out with a new mathematical model which was based on method of internal characteristic (MIC) defining the boundary conditions such as pump-turbine, ball-valve and surge tank. In addition, the load rejection transient of a pumped storage power station was predicted and compared with field experimental data, in order to explore the characteristics of the flow discharge control mode.

MIC FOR PUMP-TURBINE

The Euler equation is the energy conversion relation with the kinematics parameters at the inlet and outlet of the runner for turbine stability conditions. But the basic parameters such as load, flow discharge, and rotational speed always change frequently in the transition. Therefore, the relationship between the flow dynamics and kinematics parameters must be established for transient conditions. With the calculation MIC for the pump-turbine unit, the influences of the geometry parameters on the kinematics parameters of hydraulic machinery are analyzed, and the nonlinear equations for these parameters and the position adjustment are set up. As long as the law of the opening change of the adjusting element with time is given, the transient rules of dynamic parameters will be obtained using numerical calculation MIC for the transient solution of the nonlinear equations.

General basic equations of hydraulic machinery

Under transient conditions, the flow in the runner of the Francis pump-turbine is shown in Figure 1 (Chang 2005).

The fluid is assumed ideal and incompressible with zero radial flow velocity. According to the theorem of the moment of momentum, the moment on the micro fluid layer is equal to the derivative of the infinitesimal momentum with respect to time:

$$dM = \rho dW \frac{d(v_u r)}{dt} \tag{1}$$

where M is the moment, ρ is the fluid mass density, W is the volume, $dW = r d\theta dm db$ is the volume of micro fluid layer, b, θ, and m are the infinitesimal thickness, angle and
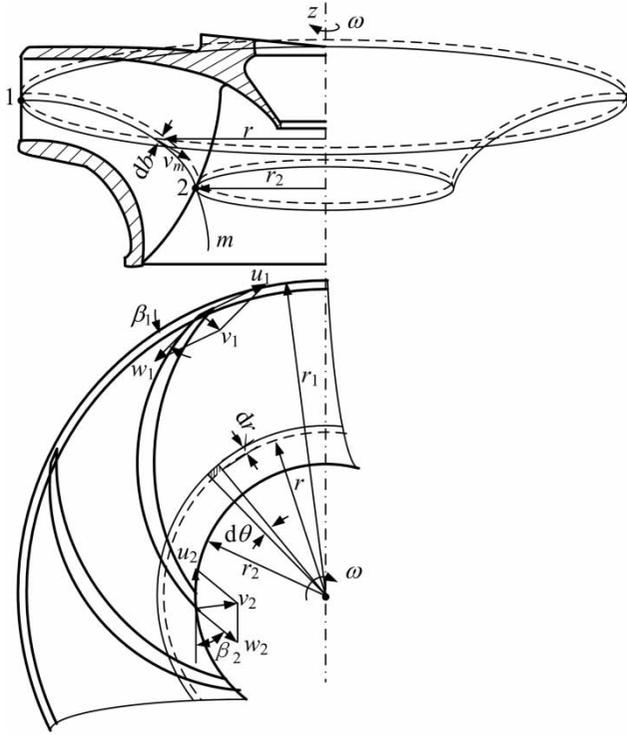
Figure 1 | Flow in pump-turbine runner (Chang 2005).

axial meridian, respectively, r is the radius of the micro fluid to the center of the shaft, v_u is the circumference component of the absolute velocity, $v_u r$ is the time-dependent velocity moment, which is related to meridian streamline and polar coordinates (m, θ), which has no relationship to the polar coordinate for axisymmetric flow. The derivative of $v_u r$ with respect to the time t, is obtained as:

$$\frac{\mathrm{d}(v_u r)}{\mathrm{d}t} = \frac{\partial(v_u r)}{\partial t} + \frac{\partial(v_u r)}{\partial m} v_m \qquad (2)$$

where $v_m = Q/(2\pi r d b)$ is the axial meridian velocity, and Q is the flow discharge.

With the substitution of Equation (2) into Equation (1), the moment on the micro fluid layer is expressed as:

$$\mathrm{d}M = \rho \mathrm{d}W \left[\frac{\partial(v_u r)}{\partial t} + \frac{\partial(v_u r)}{\partial m} v_m \right] \qquad (3)$$

Integrating Equation (3) over the volume of the micro fluid layer, the moment on the runner is expressed as:

$$M = \iiint_W \rho \left[\frac{\partial(v_u r)}{\partial t} + \frac{\partial(v_u r)}{\partial m} v_m \right] \mathrm{d}W \qquad (4)$$

Inserting the expression v_m and $\mathrm{d}W$ into the second of Equation (4), we get:

$$M = \rho \iiint_W \frac{\partial(v_u r)}{\partial t} \mathrm{d}W + \rho \iiint_W \left(\frac{\partial(v_u r)}{\partial m} \frac{Q}{2\pi r \mathrm{d}b} \right) r \mathrm{d}\theta \mathrm{d}m \mathrm{d}b$$
$$= \rho \iiint_W \frac{\partial(v_u r)}{\partial t} \mathrm{d}W + \rho Q (v_{u2} r_2 - v_{u1} r_1) \qquad (5)$$

where v_{u1} and v_{u2} are the circumference components of the absolute velocities at the inlet and outlet, respectively, r_1 and r_2 are the inlet and outlet radius of pump-turbine, respectively.

The runner is composed of many rotary surface fluid layers. Based on the relationship between acting force and reacting force, fluid transient moment acting on the runner, M_H, is then obtained as:

$$M_H = \rho Q_H (v_{u1} r_1 - v_{u2} r_2) - \rho \iiint_W \frac{\partial(v_u r)}{\partial t} \mathrm{d}W \qquad (6)$$

where Q_H is transient flow discharge.

The turbine transient water head, H_H, is obtained as:

$$H_H = \frac{M_H \omega_H}{\rho g Q_H \eta} \qquad (7)$$

where g is the gravitational acceleration, η is the hydraulic efficiency, and ω_H is the transient angular speed.

The turbine transient effective water head, H_{eH}, is obtained as:

$$H_{eH} = \eta H_H = \frac{v_{u1} u_1 - v_{u2} u_2}{g} - \frac{\omega_H}{g Q_H} \iiint_W \frac{\partial(v_u r)}{\partial t} \mathrm{d}W \qquad (8)$$

where u_1 and u_2 are the circumference velocities at the inlet and outlet, respectively.

The first item of Equation (8) is the turbine effective water head expressed by the runner transient parameters of the pump-turbine. The second item is the additional pressure, which considers the fluid inertia in the runner for transient conditions. Under steady conditions, the second items of Equations (6) and (8) are both zero, so the moment and effective water head in the runner under

steady conditions are obtained as:

$$M = \rho Q(v_{u1}r_1 - v_{u2}r_2) \tag{9}$$

$$H = \frac{v_{u1}u_1 - v_{u2}u_2}{g} \tag{10}$$

Equation (10) is the basic equation of water-turbine showing the conversion relationship between the flow energy and the mechanical energy. First, flow channel forces the fluid moment of momentum to change. Second, the fluid transmits the energy on the runner by the force on blades. Equation (10) is also called the Euler equation, building the relationship between the energy conversion and the basic flow kinematics parameters at the runner inlet and outlet under steady conditions. The Euler equation states that the energy conversion condition is the velocity moment at inlet and outlet of runner change.

The Euler equation is only applicable to the steady operations of the turbine. In the load rejection transient, the flow discharge and the rotational speed of the unit change dynamically and lead to non-zero value in the second item of Equation (8). At this time, the Euler equation is no longer applicable, especially for transient operations of the turbine, the operation parameters such as the flow velocity and the rotational speed of the unit change greatly with time because the second item is comparable to the first item and cannot be omitted. The transient moment and transient water head must be solved by Equations (6) and (8) which are called the generalized basic equations. Equations (9) and (10) are special cases of Equations (6) and (8), which are the basic expressions of transient moment and transient effective head for turbine, respectively.

The working state of the unit under pump condition is opposite to the state under turbine condition. As long as a minus sign is added to the right parts, Equations (6) and (8) will be the transient moment and the transient effective water head under pump condition. Equations (6) and (8) are also called the basic equations of hydraulic machinery, and are applied both under steady and unsteady conditions, especially under the transient for the unit.

The characteristic equation of rotating circular cascade reads:

$$\Gamma_2 = K_p\Gamma_1 + (1 - K_p)i_0 q + (1 - K_p)2\pi r_a^2 \omega \tag{11}$$

$$\Gamma_1 = 2\pi r_1 v_{u1} = \frac{\cot\alpha}{b_0}Q \tag{12}$$

where Γ_1 and Γ_2 are the velocity circulations at inlet and outlet, α is the angle between the outlet of guide vane and the circumferential direction, b_0 is the height of guide vane, $K_p = \mathrm{e}^{-(\pi l/tc)}$ is the cascade transparent coefficient, l and t_c are the length and pitch of the hydrofoil of the cascade, respectively, r_a is the effective radius of the runner cascade, $i_0 = -2\pi r_2 \cot\beta_2/F_2$ is the coefficient of the cascade in zero lift force, β_2 is the blade angle at the outlet on the meridian plane of the runner, F is the area, $q = 2\pi r v_r$ is the flow discharge of layer thickness, $v_r = Q/F$ is the radial component of the absolute velocity, and ω is the angular speed of the unit.

The cascade solidity l/t_c is large for pump-turbine, so $K_p \approx 0$ and $r_a \approx r_2$. Inserting Equation (12) into Equation (11), the difference between the velocity circulation at inlet and outlet of the cascade for pump-turbine is expressed as:

$$\Gamma_1 - \Gamma_2 = \left(\frac{\cot\alpha}{b_0} + \frac{2\pi r_2 \cot\beta_2}{F_2}\right)Q - 2\pi\omega r_2^2 \tag{13}$$

Considering $\Gamma_2 = 2\pi r_2 v_{u2}$, the difference between velocity moment at the inlet and the outlet of the runner is expressed as:

$$v_{u1}r_1 - v_{u2}r_2 = \frac{\Gamma_1 - \Gamma_2}{2\pi} \tag{14}$$

Inserting Equation (14) into Equation (6), the transient moment of pump-turbine is expressed as:

$$M_H = \rho Q_H[(\frac{\cot\alpha}{2\pi b_0} + \frac{r_2 \cot\beta_2}{F_2})Q_H - \omega_H r_2^2] - \rho \iiint\limits_W \frac{\partial(v_u r)}{\partial t}\mathrm{d}W \tag{15}$$

Motion equations of rotating parts

The working state of the unit is determined by the algebraic summation of the driving moment M_D and resisting moment M_R, namely:

$$M = \pm M_D \mp M_R = J\frac{d\omega_H}{dt} \tag{16}$$

where $J = GD^2/(4\,g)$ is the inertia moment of the rotating parts, G is the weight of the rotating parts, D is the distance from the center of mass of the rotating parts to the axle.

As shown in Figure 2, the load rejection process of the pump-turbine unit is composed of turbine, turbine-braking, and reverse pump modes. Then, the moment M is obtained by using Equation (16) and Figure 2.

Turbine mode

The pump-turbine works in a turbine mode when M_D is positive, and the motor-generator works in a generator mode when M_R is negative, where M_R only represents the mechanical friction resistance moment because the generator is not connective with the grid under load rejection condition. Meanwhile, M_R is too small and can be ignored, so the angular speed is expressed as:

$$\omega_H = \omega_0 + \frac{1}{J}\int_0^t M_D dt \tag{17}$$

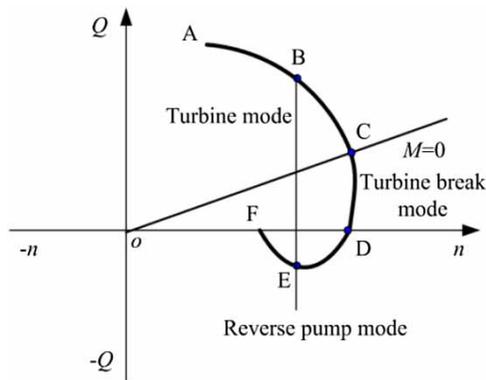where ω_0 is the initial angular speed.

Turbine-braking mode

When the driving moment equals the resisting moment, the rotational speed reaches the extremum which is named after a runaway speed. After the extremum, the pump-turbine is in turbine-braking mode and the flow discharge is small. Previous tests showed that the secondary flow loss in the runner is biggest under the condition of zero flow discharge or nearly zero flow discharge, when the brake moment caused by the secondary circumfluence is 100–4,000 times as much as that caused by the disk friction and cannot be neglected. Mockridge gave the relation curve between the shaft power coefficient K and the ratio of the blade width b_p to the runner diameter at outlet D_p under zero flow discharge condition in 1943 (Stepanoff 1993), as shown by the dotted line 1 in Figure 3. Yu (1998) gave the relation curve between K and b_p/D_p of Chinese pumps, which is shown by the solid line 2 in Figure 3, and also presented the fitting equation:

$$K = 583.312\left(\frac{b_p}{D_p}\right)^4 - 662.252\left(\frac{b_p}{D_p}\right)^3$$
$$+ 243.949\left(\frac{b_p}{D_p}\right)^2 + 2.6204\left(\frac{b_p}{D_p}\right) + 0.308874 \tag{18}$$

Under condition of near zero flow discharge, the Mockridge moment is much bigger than the other resistance moments which can be ignored. Here, the Mockridge moment M_M is written as:

$$M_M = M_R = \frac{3Kn^2 D_p^5 \times 10^{-5}}{\pi} \tag{19}$$

where n is the rotational speed of the unit.

Figure 2 | Transient process line under load rejection condition for pump-turbine (Chang 2005).
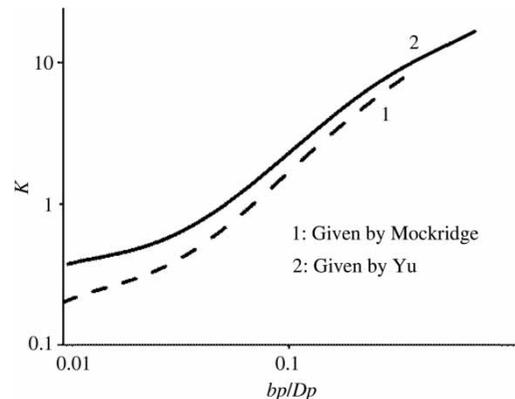

Figure 3 | Mockridge shaft power coefficient K against b_p/D_p (Stepanoff 1993; Yu 1998).

Under the same b_p/D_p, the K obtained by Yu (1998) is larger than that obtained by Mockridge. The main reason is that the braking torque obtained by Yu (1998) was drawn from the statistical methods, and thus it includes the mechanical torque. The Mockridge curve considered the secondary flow further by theoretical analysis, and thus is more appropriate for pump mode. In the transient process, the fluid flow in the pump-turbine runner is complex, and the secondary flow is serious. At the same time, the Mockridge curve obtained by theoretical analysis is more universal. Therefore, the Mockridge curve is employed during transient simulation.

In turbine-braking mode, the angular speed is expressed as:

$$\omega_H = \omega_0 + \frac{1}{J}\int_0^t (M_D - M_R)\mathrm{d}t \tag{20}$$

Reverse pump mode

When the flow discharge is less than zero, the unit is under the reverse pump condition and the moment M_D on the runner acted by water becomes resistant and is replaced by $-M_D$. The motor-generator works in a motor mode. Then, under the reverse pump condition, the angular speed is expressed as:

$$\omega_H = \omega_0 + \frac{1}{J}\int_0^t (-M_D + M_R)\mathrm{d}t \tag{21}$$

Although the proposed method in the present study is confined in a pipeline with a pump-turbine, it can easily be extended for simulation of transients in the hydraulic system with water turbine or pump as long as the flow direction and the signs of the torque and the head are changed accordingly.

The MIC expressions are based on the generalized equations of hydraulic machinery under unstable conditions, such as transient moment, transient water head, and transient axial force. The MIC can be used to calculate accurately the dynamic process of the turbine prototype device because it includes dynamic additional terms caused by the water inertia in the runner. The

transition calculation can be completed without the full characteristic curve of the vane type hydraulic machinery. Thus, the MIC expressions can be used to determine the key structure parameters during the feasibility study and preliminary technological design stages for the hydropower stations, especially for large hydropower stations which have no complete characteristic curves. At the same time, the method of combining the MIC with the characteristic line theory of pressure transients in elastic piping systems is much simpler than the traditional method based on the complete characteristic curve of hydraulic turbines because the interpolation of the complete characteristic curve is necessary for traditional methods.

NEW MODEL OF LOAD REJECTION BASED ON MIC

The internal characteristic theory describes the transient rules of the transient head, the transient rotational speed, and the transient flow discharge (Chang 2005), and then the related MIC together with the MOC defines the boundary condition of the pump-turbine system. Figure 4 is the schematic layout of two units sharing the same division pipeline, which consists of an upper reservoir, diversion tunnel, ball-valve, tailrace branches, downstream surge tank, tailrace tunnel, and downstream reservoir. The pipeline system consists of nine parts which are labeled l_1 to l_9. Water flows from upstream reservoir (Node A), through the pipeline $l1$ to the Node B, and then it is divided into
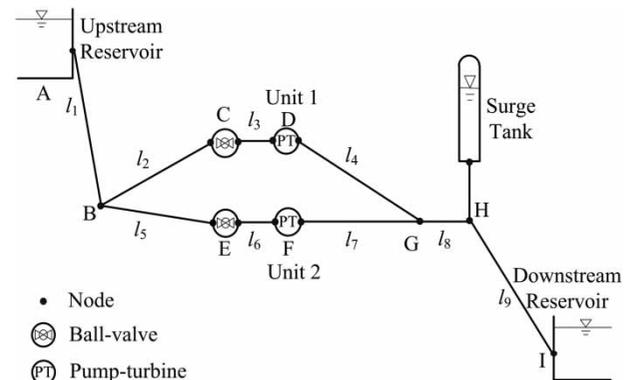

Figure 4 │ Schematic layout of two units sharing the same division pipeline.

two branches which meet at Node G. After that, it flows through the pipeline *l*8, the surge tank (Node H) and the pipeline *l*9 into the down reservoir (Node I). One branch is composed of pipelines *l*2–*l*4, the valve (Node C) and the unit 1 (Node D), the other is composed of pipelines *l*5–*l*7, the valve (Node E) and the unit 2 (Node F). The boundary conditions are set as follows.

Boundary condition of upstream reservoir

The mathematical models of the method of MOC for the upstream reservoir (Node A in Figure 4) are:

$$
\begin{cases}
H_{P1,1} = Y_{ul} \\
Q_{P1,1} = \dfrac{Y_{ul} - C_{M1}}{B_1} \\
C_M = H_{i+1} + BQ_{i+1} + RQ_{i+1}|Q_{i+1}| \\
B = \dfrac{a_w}{gA}
\end{cases}
\tag{22}
$$

where Y_{ul} is the water level of the upstream reservoir, the subscript i is the section number, a_w is the wave velocity, A is the cross-sectional area of the pipe, H_P and Q_p are the transient water head and flow discharge in P point, respectively, where the first subscript is the pipeline number and the second subscript is the section number of the pipe.

Boundary condition of branch pipes

The mathematical models of MOC for the branch pipes (Node B in Figure 4) are:

$$
\begin{cases}
H_{P1,n+1} = H_{P2,1} = H_{P5,1} \\
Q_{P1,n+1} = Q_{P2,1} + Q_{P5,1}
\end{cases}
\tag{23}
$$

Boundary condition of ball-valve

With the transient flow discharge equation based on MIC, the ball-valve is simulated as an ordinary hydraulic component with hydraulic resistance. The mathematical models of MOC for the ball-valve (Node C in Figure 4)

are:

$$
\begin{cases}
H_{P2,n+1} = C_{P2} - B_2 Q_{P2,n+1} \\
H_{P3,1} = C_{M3} + B_3 Q_{P3,1} \\
Q_{P2,n+1} = Q_{P3,1} = Q_P \\
Q_P = Q_{cb}\sqrt{1+\xi} = Q_{cb}\sqrt{\dfrac{H_{P2,n+1}}{H_{v0}}} \\
C_P = H_{i-1} + BQ_{i-1} - RQ_{i-1}|Q_{i-1}| \\
R = \dfrac{f\Delta x}{2gA^2 D}
\end{cases}
\tag{24}
$$

where H_{v0} is the initial pressure at the inlet of the ball-valve at full opening, ξ is the pressure rising rate, Q_{cb} is the static flow discharge of the ball-valve, Δx is the space increment, and f is the Darcy–Weisbach friction factor.

Boundary condition of pump-turbine (MIC)

Generally, during the load rejection process, the pump-turbine can track all the three operating conditions. Calculation formulas of corresponding transient moment and transient flow discharge based on MIC for different operating conditions are presented (Node D and Node F in Figure 4).

Turbine mode

The mathematical models of MOC for the pump-turbine under turbine operation condition are:

$$
\begin{cases}
Q_H = Q_c\sqrt{\dfrac{H_{zP}}{H_{z0}}} + D_1^3 k_q\left(n_H - n_0\sqrt{\dfrac{H_{zP}}{H_{z0}}}\right) \\
H_P = C_P - BQ_H \\
H_{zP} = H_P - H_0 + H_{z0}(1 + \sigma_T) \\
\omega_H = \omega_0 + \dfrac{1}{J}\displaystyle\int_0^t M_H \mathrm{d}t \\
M_H = \rho Q_H\left[\left(\dfrac{\cot\alpha}{2\pi b_0} + \dfrac{r_2\cot\beta_2}{F_2}\right)Q_H - \omega_H r_2^2\right]
\end{cases}
\tag{25}
$$

where $Q_c = Q_0 y^k$ is the static flow discharge, Q_0 is the static flow discharge at full opening of the guide vane, $y = a/a_0$ is the relative opening of the guide vane, a is the opening of the guide-vane, a_0 is the full opening of the guide vane, k is the exponent which is dependent on the classification of turbine and the specific speed of turbine, H_{zp} is the transient water

head of the device, H_{z0} is the static water head of the device, D_1 is the runner diameter of pump-turbine, $n_H = \omega_H r$ is the transient rotational speed, n_0 is the initial rotational speed, k_q is the rate of change of unit discharge with respect to unit speed and is determined by specific speed, $k_q < 0$, when pump-turbine is in a turbine mode, H_0 is the static water head at the spiral case inlet, $\sigma_T = L_{dr} v_{dr}/(g H_{z0} t_s)$ is the characteristic coefficient of the draft tube, L_{dr} is the length of the draft tube, v_{dr} is the initial average velocity in the draft tube, t_s is the closing time of the guide vane, and b_0 is the height of the guide vane.

Turbine-breaking mode

The mathematical models of MOC for pump-turbine under turbine-breaking operation condition are:

$$
\begin{cases}
Q_H = K_1 \left(\dfrac{n_H D_1}{\sqrt{H_{zP}}} - \dfrac{60}{\sqrt{c_1 - c_2 x}} \right) D_1^2 \sqrt{H_{zP}} \\
H_P = C_P - B Q_H \\
H_{zP} = H_P - H_0 + H_{z0}(1 + \sigma_T) \\
\omega_H = \omega_0 + \dfrac{1}{J} \displaystyle\int_0^t (M_H - M_R)\,\mathrm{d}t \\
M_H = \rho Q_H \left[\left(\dfrac{\cot\alpha}{2\pi b_0} + \dfrac{r_2 \cot\beta_2}{F_2} \right) Q_H - \omega_H r_2^2 \right] \\
M_R = \dfrac{3 K n_H^2 D_1^5 \times 10^{-5}}{\pi}
\end{cases}
\tag{26}
$$

where K_1 is the iterative coefficient, c_1 and c_2 are both coefficients associated with specific speed.

Reverse pump mode

The mathematical models of MOC for pump-turbine under reverse pump operation condition are:

$$
\begin{cases}
Q_H = K_2 \left(\dfrac{n_H D_1}{\sqrt{H_{zP}}} - \dfrac{60}{\sqrt{c_1 - c_2 x}} \right) D_1^2 \sqrt{H_{zP}} \\
H_P = C_P - B Q_H \\
H_{zP} = H_P - H_0 + H_{z0}(1 + \sigma_T) \\
\omega_H = \omega_0 + \dfrac{1}{J} \displaystyle\int_0^t (M_R - M_H)\,\mathrm{d}t \\
M_H = \rho Q_H \left[\omega_H r_2^2 - \left(\dfrac{\cot\alpha}{2\pi b_0} + \dfrac{r_2 \cot\beta_2}{F_2} \right) Q_H \right] \\
M_R = \dfrac{3 K n_H^2 D_1^5 \times 10^{-5}}{\pi}
\end{cases}
\tag{27}
$$

where K_2 is the coefficient associated with specific speed.

Boundary condition of parallel pipes

The mathematical models of MOC for the parallel pipes (Node G in Figure 4) are:

$$
\begin{cases}
H_{P4,n+1} = H_{P7,n+1} = H_{P8,1} \\
Q_{P8,1} = Q_{P4,n+1} + Q_{P7,n+1}
\end{cases}
\tag{28}
$$

Boundary condition of downstream surge tank

The mathematical models of MOC for the surge tank are (Node H in Figure 4):

$$
\begin{cases}
Q_T = Q - Q_S \\
\dfrac{h_S}{g A_S} \dfrac{\mathrm{d}Q_S}{\mathrm{d}t} = H_{ds} - H_{s0} - \dfrac{f_S |Q_S| Q_S}{2 g D_S A_S^2} - \dfrac{|Q_S| Q_S}{g A_S^2} \\
H_{P8,n+1} = H_{P9,1} \\
H_{P8,n+1} = C_{P8} - B_8 Q_T \\
H_{P9,1} = C_{M9} + B_9 Q
\end{cases}
\tag{29}
$$

where Q_T is the flow discharge at the outlet of the downstream surge tank, Q_S is the flow discharge of the downstream surge tank, h_S is the depth of the downstream surge tank, H_{dS} is the water head of the downstream surge tank, HS_0 is the water head at the bottom of the downstream surge tank, f_S is the friction factor of the downstream surge tank, D_S and A_S are the diameter and cross-sectional area of the downstream surge tank, respectively.

Boundary condition of downstream reservoir

The mathematical models of MOC for the downstream reservoir (Node I in Figure 4) are:

$$
\begin{cases}
H_{P9,n+1} = Y_{dl} \\
Q_{P9,n+1} = \dfrac{C_{M9} - Y_{dl}}{B_9}
\end{cases}
\tag{30}
$$

where Y_{dl} is the water level of the downstream reservoir.

Numerical method for solving MIC equations

The transient process is calculated as the unit operation conditions, and the ball-valve closing law and the guide vane

closing law are given. The solving processes for the pump-turbine and the ball-valve using the MIC are briefly described as follows: (1) according to the closing laws of the guide vane and ball-valve, the initial steady angular speed of the unit is determined; (2) the steady flow inside the ball-valve is determined; (3) according to the movement of the guide vane, the steady flow inside the unit is calculated, and then the transient flow discharge is obtained; (4) the values of dq/dt and $d\omega/dt$ are calculated, where the linear interpolations of dq/dt and $d\omega/dt$ are adopted; (5) the transient torque is calculated; (6) the steady angular speed and transient angular speed are calculated, respectively; (7) the calculated angular speed is compared with the initial value. If the error does not meet the requirement, the calculated value will be taken as the initial value to calculate again until the value meets the requirement.

The MOC is employed to solve the equations along the characteristic line, where the central difference scheme is used for the flow discharge term and the pressure term and the trapezoidal integration method adopted for the rotational speed. The upstream reservoir is calculated by $C-$ equation and the downstream reservoir is solved by $C+$ equation because the water level is constant for large reservoirs. Based on the above equations, the load rejection transition process is calculated by applying the MIC and MOC.

CASE STUDIES AND ANALYSES

Basic parameters of pump-turbine units

The numerical simulation of a simultaneous load rejection process of two units based on MIC was carried out in this paper. The field data of the load rejection transients, which were obtained from the pumped storage power station, were employed to validate the above-mentioned relevant models and methods. The numerical simulation of a simultaneous load rejection process of two units with nominal net head was compared with a field test. The schematic layout of the division pipeline is given in Figure 4. The basic characteristics of these two pump-turbine units are given in Table 1 and the parameters before load rejecting in Table 2. The flow discharge was regulated by the ball-valve and guide

Table 1 | Basic parameters of pump-turbine units

Parameter	Value
Flow discharge (m³/s)	80.1
Nominal net head (m)	308
Turbine output (MW)	306.12
Rotational speed (r/min)	333.3
Runner diameter (m)	4.565
Guide vane number	20
Guide vane height (m)	0.5714

vane in the load rejection transient process. Figure 5 shows the closing laws of the guide vane and the ball-valve. During the first 11 seconds of the load rejection transient process, the guide vane was in the original position. From 11 to 26 seconds, the guide vane was closed linearly to zero opening from the initial opening. Finally, the guide vane was at zero opening. During the first 60 seconds of the load rejection transient process, the ball-valve was closed linearly to zero opening from the original position. Finally, the ball-valve was at zero opening.

Measured and predicted data

Figures 6 and 7 show the water hammer data which were measured and predicted for unit 1 and unit 2 during the simultaneous load rejection process of the two units, respectively. At the beginning stage (0–10 s), the pressure at the spiral case inlet increased and that at the draft tube inlet decreased because of the rapid decrease of the discharge inside the runner, which was caused mainly by the centrifugal effect of the flowing fluid inside the runner of

Table 2 | Key parameters before load rejection process

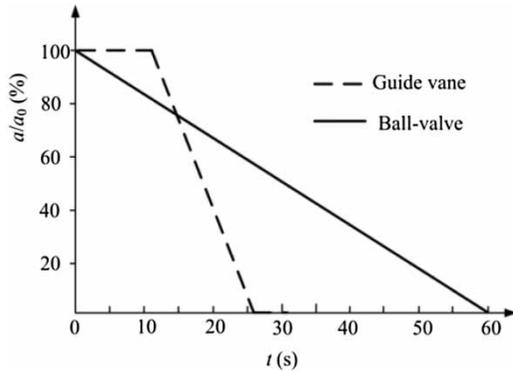| Parameter	Value
Output (MW)	300
Flow discharge (m³/s)	98.14
Water head (m)	328
Rotational speed (r/min)	333.3
Guide vane closing time (s)	26
Guide vane delay time (s)	11
Ball-valve closing time (s)	60

Figure 5 | Closing laws of the guide vane and ball-valve.

the pump-turbine during the rise of the rotational speed. When the change of the discharge reached the maximum, the pressure rose to the first extremum (point D) which lagged nearly 3 seconds behind the occurring time of the maximum rotational speed, because the centrifugal effect reached the maximum when the rotational speed reached extreme value while the discharge drop caused by the ball-valve was not large due to the slow change of flow area of the ball-valve at its large opening. Then, the pressure at the spiral case inlet dropped to the extremum (point E) and the pressure at the draft tube inlet rose to the maximum
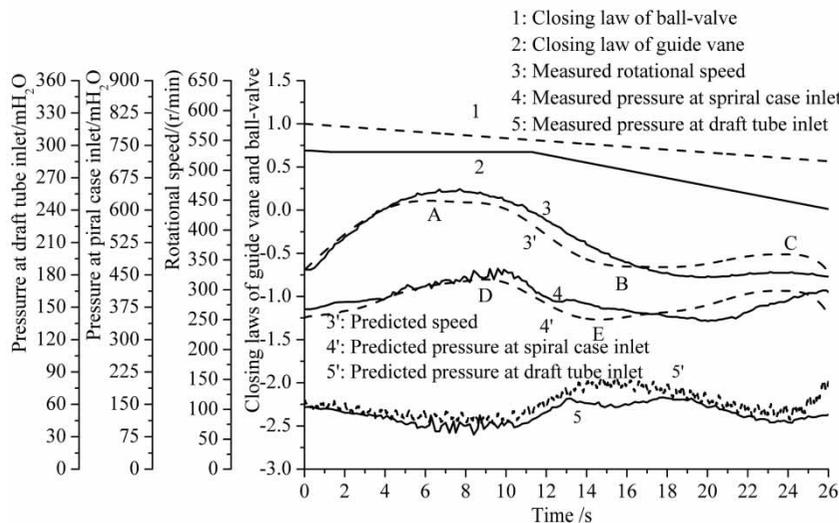
Figure 6 | Measured and predicted water hammer curves of unit 1 during simultaneous load rejection process of two units.
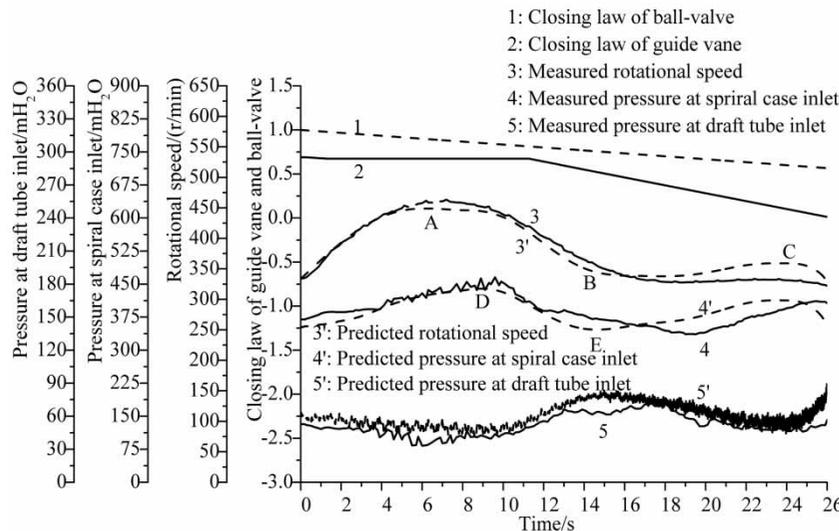

Figure 7 | Measured and predicted water hammer curves of unit 2 during simultaneous load rejection process of two units.

because the change of the discharge decreased, which was caused by the coupling effect of both the ball-valve and the rotational speed. After that, the pressure at the spiral case inlet increased again to the second maximum because the discharge decreased, which was caused by the guide vane closing. However, the first extremum was larger than the second extremum, which indicated that the centrifugal effect was obvious for the pump-turbine with low specific speed. Henceforth, the pressure fluctuations began to flatten out due to the resistance of the pipeline.

Analyses of measured and predicted data

It can be seen from Figures 6 and 7 that the predicted pressure at the spiral case inlet was in good agreement with the experimental data at the beginning of the pressure rising process. The predicted maximum pressure at the spiral case inlet (point D) appeared nearly 1 second ahead of the occurring time of the measured maximum, and the predicted minimal pressure at the spiral case inlet (point E) appeared nearly 5 seconds ahead of the occurring time of minimum measured value, because the rotational speed rise caused the decrement of flow discharge and the pressure pulsation at the spiral case inlet changed with the discharge. The change trend of the predicted pressure at the draft tube inlet was similar to the measured one, but there was a little difference between the predicted and the measured extremums. The measured and predicted minimum relative pressures at the draft tube inlet of unit 1 were 25.6% and 18.9%, respectively, and the corresponding values of unit 2 were 25.86% and 18.88%, respectively. The relative errors of the maximum rise of hydraulic pressure at the spiral case inlet were −6.7% and −6.98%, respectively. The measured and predicted minimum absolute pressures at the draft tube inlet of unit 1 were 32.03 mH$_2$O and 39.59 mH$_2$O, respectively, and the corresponding values of unit 2 were 33.13 mH$_2$O and 41.74 mH$_2$O, respectively. The relative errors of the maximum rise of hydraulic pressure were 7.56% and 8.61%, respectively.

During the first 7 seconds of the load rejection process, the rotational speed of the unit had been rising because the driving moment of the fluid acting on the runner was greater than the resisting moment, and at this time, the pump-turbine unit worked in a turbine mode. When the driving moment equaled the resisting moment, the rotational speed reached the first extremum (point A) which appeared nearly 4 seconds ahead of the start time of the guide vane closing. Then, the unit operation moved into turbine-breaking mode and the rotational speed started to decrease to the extremum (point B), which was caused by the braking moment and the hydraulic moment due to the positive water hammer. Henceforth, the rotational speed gradually fluctuated to zero because of the joint actions of the above-mentioned two types of moments.

At the beginning of the rotational speed rising process, the predicted rotational speed was close to the experimental data. The maximum relative rotational speeds of the predicted and the predicted results of unit 1 were 40.6% and 34.7%, respectively, and the corresponding values of unit 2 were 39.1% and 34.66%, respectively. The relative errors of the maximum rotational speed of the two units between the predicted results and the experimental data were −5.9% and −4.44%, respectively. After the rotational speed reached the maximum, the predicted rotational speed decreased rapidly and the minimum of the predicted rotational speed (point B) appeared nearly 3 seconds ahead of the minimum of the measured rotational speed. The second extremum of the predicted rotational speed (point C) was bigger than the measured one in turbine-breaking mode because the Mockridge moment was possibly added on the runner earlier during the transient process. Thus, it is very important to investigate the suitable time to add the Mockridge moment when using the MIC in the future.

Figure 8 shows the field experimental curves for unit 1 and unit 2 during the simultaneous load rejection process of the two units. The change trend of water hammer data was similar for unit 1 and unit 2, because these two pump-turbine units had the same basic characteristics and similar hydraulic conditions which led to similar pressure pulsations and rotational speed rising. There was a little difference between the change curves of water hammer data including the phase and amplitude because the tailrace branch of unit 1 was much longer than unit 2.

In order to carry out clearer comparisons, the predicted and the measured extremums of two units during the simultaneous load rejection process of the two units are summarized in Table 3. The absolute errors of the maximum rotational speed and the maximum pressure at the spiral
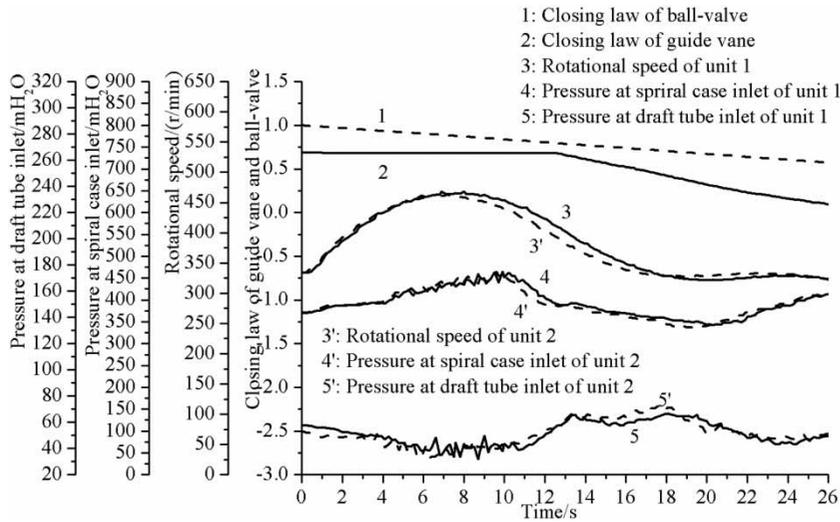
Figure 8 | Experimental curves of unit 1 and unit 2 during simultaneous load rejection process of two units.

case inlet were both small, while the absolute error of the pressure at the draft tube inlet was relatively large. The maximum pressures at the spiral case inlet were far less than the maximum allowed value (500 mH$_2$O), and the minimum pressures at the draft tube inlet were larger than the minimum allowed value (20 mH$_2$O). The maximum of the rotational speed rise ratios was less than the maximum allowed value (45%). Thus it was concluded that the joint

closing law of ball-valve and guide vane for two units could prevent the pressure pulsation and the rotational speed rise effectively.

The computational relative errors including the rotational speed and the pressures at the spiral case inlet for the two units were calculated from the time of initial load rejection to 26 seconds, as shown in Figure 9. All the errors were small at the beginning of load rejection and became a little larger in the later stage. Those were all within the allowable range. The main reasons were that the flow was extremely complex when the units were in

Table 3 | Predicted and measured extremums during simultaneous load rejection process of two units

Parameter	Unit	Measured	Predicted	Absolute error
Maximum rotational speed				
Absolute value (r/min)	1	468.66	449.01	−19.65
	2	463.59	448.87	−14.72
Rise ratio value (%)	1	40.6	34.7	−5.9
	2	39.1	34.66	−4.44
Maximum pressure at spiral case inlet				
Absolute value (mH$_2$O)	1	464.35	439.54	−24.81
	2	465.32	439.52	−25.8
Rise ratio value (%)	1	25.6	18.9	−6.7
	2	25.86	18.88	−6.98
Minimum pressure at draft tube inlet				
Absolute value (mH$_2$O)	1	32.03	39.59	7.56
	2	33.13	41.74	8.61

Absolute error = predicted value − measured value; rise ratio = (predicted (or measured) value − initial value) / initial value.
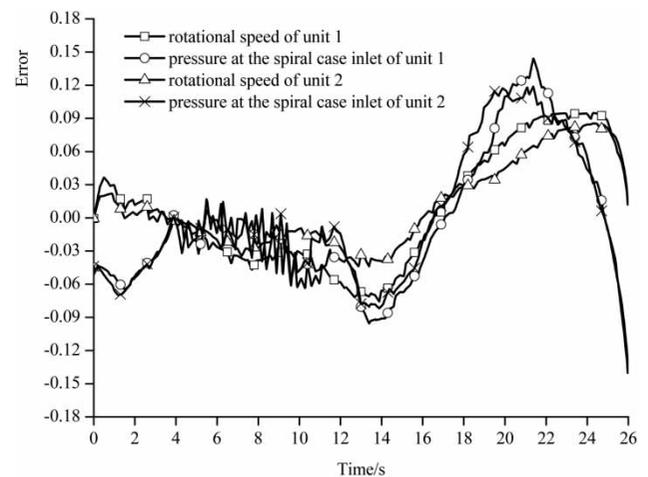

Figure 9 | Computational errors between predicted and measured rotational speed and pressure at the spiral case inlet.
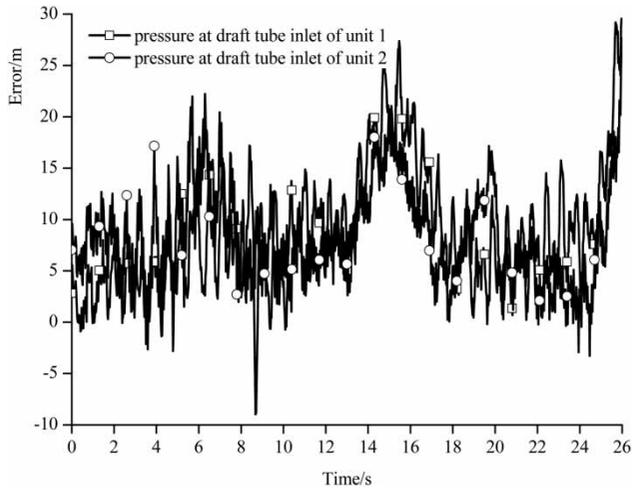
Figure 10 │ Computational errors between predicted and measured pressure at the draft tube inlet.

the anti-pump operation condition and the Mockridge moment was probably not accurate enough. The computational errors of the pressures at the draft tube inlet for the two units were also calculated from the time of initial load rejection to 26 seconds, as shown in Figure 10. The errors were a little large, but most of them were within the allowable range. The main reasons were that the vortex rope in the draft tube affected the fluid flow severely and the flow was extremely unstable in the 'S' operation region for low specific speed pump-turbine, which caused large fluctuations in the measured data.

The average computational errors, including rotational speed, pressures at the spiral case inlet and at draft tube inlet for unit 1 were 4.5%, 4.9%, and 8.7 mH$_2$O, and the corresponding root mean square errors (RMSEs) were 5.3%, 5.9%, and 9.3 mH$_2$O. The average computational errors, including rotational speed, pressures at the spiral case inlet and at draft tube inlet for unit 2 were 3.1%, 4.7%, and 8.3 mH$_2$O, and the corresponding RMSEs were 3.9%, 5.9%, and 9.1 mH$_2$O. The comparisons showed that all the average errors were closer to the experimental values than the RMSE values.

CONCLUSIONS

A new mathematical model based on MIC was proposed to simulate the transient process under the simultaneous load

rejection of two units with joint closing law of ball-valve and guide vane in a pumped storage power station. Meanwhile, the hydraulic boundary conditions of pump-turbine, and other coupling boundary conditions of the ball-valve and the guide vanes were incorporated. The main conclusions were as follows.

In the first 10 seconds of the load rejection process, the pressure at the spiral case increased gradually to the maximum value. After a decreasing process of 10 seconds, the pressure began to increase and reached the second extreme. The trend of the pressure change at the draft tube inlet was almost opposite to the trend at the spiral case inlet. At the first stage (0–7 s) of the load rejection process, the rotational speed of the unit kept rising until it reached the first extremum. Then, the rotational speed decreased to the minimum in 13 seconds. After that, it started to increase to the second extremum and then gradually fluctuated to zero. The maximum rotational speed occurred about 5 seconds ahead of the moment at which the guide vane started to close, corresponding to nearly 3 seconds ahead of the moment when the maximum pressure occurred at the spiral case inlet.

At the spiral case inlet, the first pressure extremum subjected to the rotational speed increasing was greater than the second extremum, which was caused mainly by the guide vane closing process. It indicated that the centrifugal force of the fluid inside the runner had a great influence on the transient parameters in load rejection process of the pump-turbine with low specific speed.

The measured and predicted results confirmed that the maximum rotational speeds, the maximum pressures at the spiral case inlet, and the minimum pressures at the draft tube inlet all met the design specification requirements. During the simultaneous load rejection, the change trends of the transient parameters were similar for the two units which shared the same division pipeline. The technique for controlling flow discharge based on the joint closing law of ball-valve and guide vane for two units was acceptable.

The relative errors of the predicted maximum rotational speeds and the maximum pressures of the two units agreed well with the experimental data. The above analyses and comparisons indicated that the proposed models of MIC and numerical techniques were reliable in predicting the

double load rejection process. The MIC can be used to analyze other transients of the hydraulic system with water turbine or pump as long as the signs of torque and head are changed properly.

ACKNOWLEDGEMENT

REFERENCES

Acosta, S., Puelz, C., Riviére, B., Penny, D. J. & Rusin, C. G. 2015 Numerical method of characteristics for one-dimensional blood flow. *Journal of Computational Physics* **294**, 96–109.

Calamak, M. & Bozkus, Z. 2013 Comparison of performance of two run-of-river plants during transient conditions. *Journal of Performance of Constructed Facilities* **27** (5), 624–632.

Chang, J. S. 2005 *Transient of Hydraulic Machine Installations.* Higher Education Press, Beijing, China.

Fang, Y. J. & Koutnik, J. 2012 The numerical simulation of the delayed load rejection of a pump-turbine powerplant. In: *Proceedings of the 26th IAHR Symposium on Hydraulic Machinery and Systems*, Beijing, China, pp. 2018–2026.

Freni, G., Marchis, M. D. & Napoli, E. 2013 Implementation of pressure reduction valves in a dynamic water distribution numerical model to control the inequality in water supply. *Journal of Hydroinformatics* **16** (1), 207–217.

Hou, C. S. & Cheng, Y. G. 2005 Optimized closing procedures of wicket gate and ball valve for high head reversible pump-turbine unit. *Engineering Journal of Wuhan University* **38** (3), 59–62.

Hwang, Y. H., Huang, H. S., Chung, N. M. & Wang, P. Y. 2012 Particle method of characteristics (PMOC) for unsteady pipe flow. *Journal of Hydroinformatics* **15** (3), 780–797.

Li, D., Gong, R., Wang, H., Xiang, G., Wei, X. & Qin, D. 2016 Entropy production analysis for hump characteristics of a pump turbine model. *Chinese Journal of Mechanical Engineering* **29** (4), 803–812.

Rezghi, A. & Riasi, A. 2016 Sensitivity analysis of transient flow of two parallel pump-turbines operating at runaway. *Renewable Energy* **86**, 611–622.

Stepanoff, A. J. 1993 *Centrifugal and Axial Flow Pumps: Theory, Design, and Application,* 2nd edn. Krieger Publishing Company, Malabar, FL, USA.

Vakil, A. & Firoozabadi, B. 2009 Investigation of valve-closing law on the maximum head rise of a hydropower plant. *Scientia Iranica Transaction B – Mechanical Engineering* **16** (3), 222–228.

Wylie, E. B. & Streeter, V. L. 1993 *Fluid Transient in Systems.* Prentice-Hall, Englewood Cliffs, NJ, USA.

Yao, Z., Bi, H. L., Huang, Q. S., Li, Z. J. & Wang, Z. W. 2013 Analysis on influence of guide vanes closure laws of pump-turbine on load rejection transient process. In: *Proceedings of 6th International Conference on Pumps and Fans with Compressors and Wind Turbines (ICPF2013)*, Beijing, China, pp. 66–71.

Yu, Z. M. 1998 Determination of shaft power and braking moment at zero flow condition of vane pump. *Water Conservancy and Hydropower Technology* **29** (4), 15–16.

Yu, X., Zhang, J. & Zhou, L. 2014 Hydraulic transients in the long diversion-type hydropower station with a complex differential surge tank. *The Scientific World Journal* **2014** (4), 241868.

Zeng, W., Yang, J. & Hu, J. 2017 Pumped storage system model and experimental investigations on s-induced issues during transients. *Mechanical Systems & Signal Processing* **90**, 350–364.

Zhang, C. & Yang, J. 2011 Study on linkage closing rule between ball valve and guide vane in high head pumped storage power station. *Water Resources & Power* **29** (12), 128–131.